HOMO energy levels of the porphyrin. This is evidenced by the oxidation pattern of (OEP)Fe(C_6H_5)(py) that, as indicated by time-resolved electronic absorption spectra, involves both spin-coupled iron(III) radical cation and iron(IV) porphyrin cation forms.

In summary we have shown that pyridine coordinates to oxidized, neutral, and reduced iron(III)–phenyl σ-bonded five-coordinate porphyrins producing the corresponding six-coordinate derivatives. This coordination results in stabilization of the neutral and oxidized species. Also we report the first case where oxidation and reduction of the same iron(III) porphyrin can be described as occurring at a location involving both the central metal orbitals and those of the π ring system. These electrochemical reactions can be described by a mixed formalism involving an Fe(IV) complex and an Fe(III) cation radical, as well as an Fe(II) complex and an Fe(III) anion radical.

Acknowledgment. The support of the National Institutes of Health (GM 25172) is gratefully acknowledged.

Registry No. (OEP)Fe(C_6H_5)(py), 90148-87-1; (TPP)Fe(C_6H_5)(py), 90148-88-2; (OEP)Fe(C_6H_5), 83614-06-6; (TPP)Fe(C_6H_5), 70936-44-6; [(OEP)Fe(C_6H_5)(py)]$^+$, 90148-89-3; [(TPP)Fe(C_6H_5)(py)]$^-$, 90148-90-6.

Bridged Ferrocenes. 10.[1] Structural Phenomena

Manny Hillman,* Etsuko Fujita, and Helen Dauplaise

Chemical Science Division, Department of Applied Science, Brookhaven National Laboratory, Upton, New York 11973

Åke Kvick

Department of Chemistry, Brookhaven National Laboratory, Upton, New York 11973

Robert C. Kerber

Department of Chemistry, State University of New York at Stony Brook, Stony Brook, New York 11797

Received February 21, 1984

The structures of 1,1′,2,2′-bis(tetramethylene)ferrocene, I, 1,1′,2,2′,4,4′-tris(tetramethylene)ferrocene, II, and 1,1′,2,2′,4,4′-tris(pentamethylene)ferrocene, III, are given and are compared to the previously determined[2] structure of 1,1′,2,2′,4,4′-tris(trimethylene)ferrocene, IV. The iron-to-ring distances are consistent with the reported Mössbauer spectra[3] and redox potentials.[4] The cyclopentadienyl rings are eclipsed in the compounds with trimethylene and pentamethylene bridges but are staggered by 12–14° in the compounds with tetramethylene bridges. In compounds with tetra- and pentamethylene bridges the presence of staggering or eclipsing is attributed to the need to avoid eclipsing of the protons in the bridges. In the compound with three trimethylene bridges, the shortness of the bridges is of primary importance. The staggered conformation observed in I and II may be the source of the apparent anomalies observed in the ring-proton region of the NMR spectra of bridged ferrocenes. The bridge-proton region of the NMR spectra at 360 MHz are given for I and other bridged ferrocenes. Disorder of the bridge carbons observed in the crystals are correlated with the flipping of the bridges observed in the NMR spectra.

Introduction

In the NMR spectra reported for the bridged ferrocenes,[5] anomalies occur. The separation of the chemical shifts of the ring protons is greater in ferrocene with a trimethylene bridge ($\Delta\delta$ = 0.05 ppm) than in ferrocene with a tetramethylene bridge ($\Delta\delta$ = 0.04 ppm). This is in accord with the observation[6-8] that greater ring tilting leads to a greater separation of the chemical shifts of the ring protons. However, in ferrocene with a pentamethylene bridge the separation of the chemical shifts of the ring protons ($\Delta\delta$ = 0.11 ppm) is greater than even in trimethyleneferrocene. Similar reversals have been reported[5] for the related compounds with two and three bridges. E.g., the ratios of the ring-proton peaks (downfield to upfield) are 2:1, 1:2, and 2:1 for V, VI, and VII (all structures are illustrated in Figures 1–5), respectively. It was anticipated that some variance in the structures of the tetramethylene and pentamethylene derivatives was responsible for these anomalies. For this reason an attempt is underway to determine the structures of relevant bridged ferrocenes. In this paper the structures of a bis(tetramethylene)-, I, a tris(tetramethylene)-, II, and a tris(pentamethylene)-ferrocene, III, are reported.

Experimental Section

Compounds I, II and III were prepared by the procedures of Hisatome et al.[5,9,10] Crystals were grown from hexane solutions and were mounted along their long axes for the collection of the diffraction intensity data.

The intensity data were collected on an Enraf-Nonius CAD-4 diffractometer with graphite-monochromated Mo Kα radiation (λ = 71.07 pm). The crystal data are given in Table I. The

(1) Paper 9 of series: Hillman, M.; Matyevich, L.; Fujita, E.; Jagwani, U.; McGowan, J. *Organometallics* **1982**, *1*, 1226–9.
(2) Hillman, M.; Fujita, E. *J. Organomet. Chem.* **1978**, *155*, 87–98.
(3) Hillman, M.; Nagy, A. G. *J. Organomet. Chem.* **1980**, *184*, 434–445.
(4) Fujita, E.; Gordon, B.; Hillman, M.; Nagy, A. G. *J. Organomet. Chem.* **1981**, *218*, 105–114.
(5) Hisatome, M.; Hillman, M. *J. Organomet. Chem.* **1981**, *212*, 217–231.
(6) Rinehart, K. L., Jr.; Frerichs, A. K.; Kittle, P. A.; Westman, L. F.; Gustafson, D. H.; Pruett, R. L.; McMahon, J. E. *J. Am. Chem. Soc.* **1960**, *82*, 4111–4112.
(7) Barr, T. H.; Watts, W. E. *Tetrahedron* **1968**, *24*, 6111–6118.
(8) Hillman, M.; Weiss, A. J. *J. Organomet. Chem.* **1972**, *42*, 123–128.
(9) Hisatome, M.; Sakamoto, T.; Yamakawa, K. *J. Organomet. Chem.* **1976**, *107*, 87–101.
(10) Hisatome, M.; Watanabe, N.; Sakamoto, T. Yamakawa, K. *J. Organomet. Chem.* **1977**, *125*, 79–93.

0276-7333/84/2303-1170$01.50/0

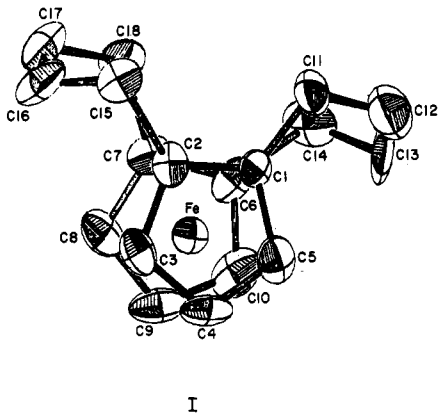

I

Figure 1. ORTEP diagram of non-hydrogen atoms of compound I. The ellipsoids represent 50% probabilities.

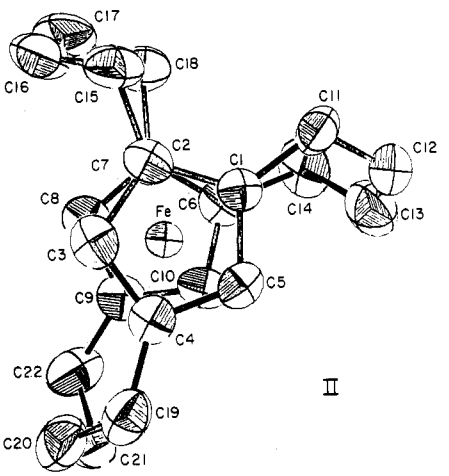

II

Figure 2. ORTEP diagram of non-hydrogen atoms of compound II. The ellipsoids represent 50% probabilities.

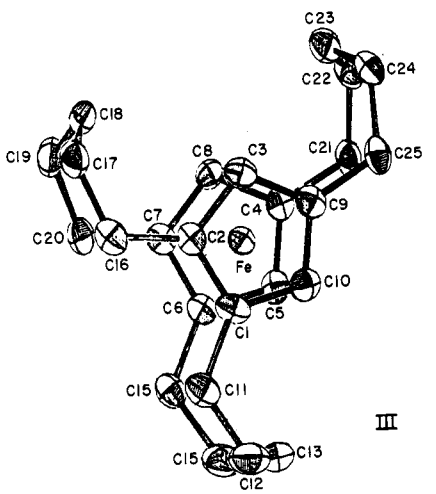

III

Figure 3. ORTEP diagram of non-hydrogen atoms of compound III. The ellipsoids represent 50% probabilities.

centrosymmetric space group of II was established from the success of the refinement. Intensities were collected by using θ–2θ scans and were corrected for Lorentz and polarization effects. Absorption corrections were performed for II.

The structures were determined by using the SHELX-76 crystallographic computing package.[11] The atomic scattering factors for iron including components for anomalous dispersion were taken from tabulations of Doyle and Turner[12] and Cromer and Liberman.[13] Those for hydrogen are from Stewart et al.[14] The other atomic scattering factors are from Cromer and Mann.[15] The iron atoms were located from Patterson maps, and the remaining atomic positions were obtained from successive difference Fourier maps.

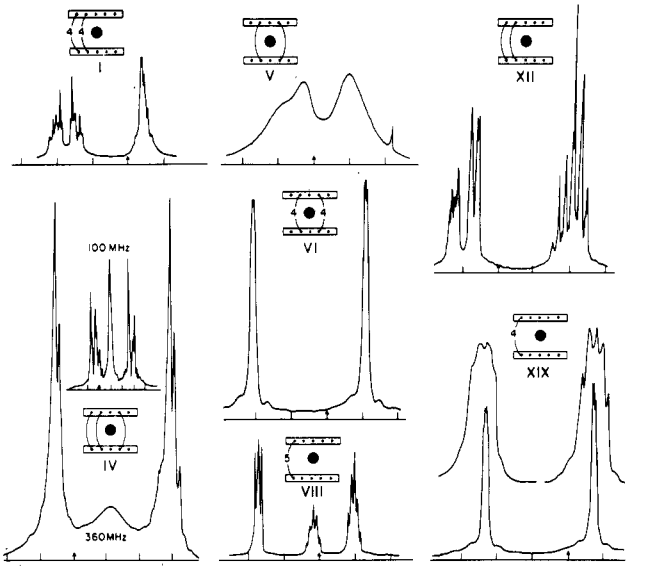

Figure 4. NMR spectra at 360 MHz of the bridge-proton region of bridged ferrocenes. The tics are separated by $\Delta\delta = 0.2$ ppm. The tics with the arrows are at δ 2.0. The scales increase to the left. In the molecular structures, the rectangles represent the cyclopentadienyl rings, the small solid circles the carbon atoms of the ring, the larger circles the iron atoms, and the arcs the bridges. The numbers embedded in the arcs are the number of methylene groups. The unlabeled arcs are trimethylene bridges. The spectrum of IV is also given at 100 MHz.

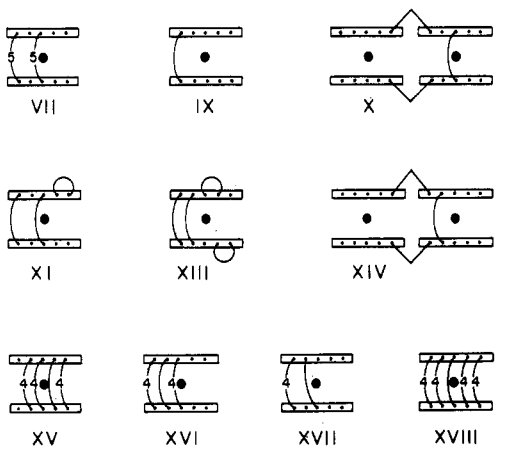

Figure 5. Representations of bridged ferrocenes as described in the caption of Figure 4.

For I and II, meaningful refinement of the coordinates of the hydrogen atoms on the bridges was not possible because of a small amount of disorder (approximately one residual electron) in the neighborhood of the β-carbon atoms of the bridges. Consequently, the coordinates of all of the hydrogen atoms were calculated following each least-squares refinement of the coordinates and anisotropic thermal parameters for the non-hydrogen atoms (full-matrix least squares in the case of I, two separate blocks for II, one for the two ferrocene units, and one for the bridges). The C–H distances were assigned as 100 pm, and the isotropic thermal parameters of the hydrogen atoms were assigned as $U = 500$ pm^2.

(11) Sheldrick, G. M. In "Computing in Crystallography"; Schenk, H., Olthof-Hazekamp, R., van Koningsveld, H., Bassi, G. C., Eds.; Delft University Press: Delft, Holland, 1978; pp 34–42.

(12) Doyle, P. A.; Turner, P. S. *Acta Crystallogr. Sect. A* **1968**, *A24*, 390–397.

(13) Cromer, D. T.; Liberman, D. *J. Chem. Phys.* **1970**, *53*, 1891–1898.

(14) Stewart, R. F.; Davidson, E. H.; Simpson, W. T. *J. Chem. Phys.* **1965**, *42*, 3175–3187.

(15) Cromer, D. T.; Mann, J. B. *Acta Crystallogr., Sect. A* **1968**, *A24*, 321–325.

Table I. Crystal Data

	I	II	III
mol formula	$C_{18}H_{22}Fe$	$C_{22}H_{28}Fe$	$C_{25}H_{34}Fe$
mol wt	294.22	348.31	390.39
2θ range for matrix, deg	10-28	29-57	25-39
space group	*Pnaa*	$P\bar{1}$	$P2_1/c$
a, pm	895.6 (5)	1013.2 (2)	1527.4 (3)
b, pm	1193.0 (3)	1337.8 (7)	712.4 (2)
c, pm	2564.1 (7)	1356.5 (4)	1761.7 (2)
α, deg	90.00	103.45 (4)	90.00
β, deg	90.00	99.22 (2)	93.27 (1)
γ, deg	90.00	102.62 (3)	90.00
V, nm^3	2.740	1.701	1.914
Z	8	4	4
ρ_{calcd}, g/cm^3	1.427	1.361	1.355
abs coeff, cm^{-1}	10.54	8.54	7.63
2θ range, deg	2-56	2-55	2-58
reflctns collected	5199	10619	6037
reflctns used ($F > 2\sigma$)	1238	6663	3003
parameters refined	172	416	371
scan width	0.7 + 0.35 tan θ	1.0 + 0.14 tan θ	0.8 + 0.35 tan θ
$R(F) = \Sigma \lvert F_o - F_c \rvert / \Sigma \lvert F_o \rvert$	0.100	0.053	0.056
$R_w(F) = \Sigma \lvert F_o - F_c \rvert w^{1/2} / \Sigma \lvert F_o \rvert w^{1/2}$	0.074	0.068	0.042
$w = 1/(\sigma^2(F) + cF^2)$, c =	0.0010	0.0072	0.0001
max shift/error (non-H)	0.14	0.21	0.11
max shift/error (H)			0.03
res electron dens, e nm^{-3}	1000	840	630

Table II. Fractional Coordinates[a] for $C_{18}H_{22}Fe$ (I)

atom	x/a	y/b	z/c	atom	x/a	y/b	z/c
Fe	8192 (2)	4057 (1)	6278 (1)	H5	946	377	725
C1	8267 (13)	5137 (9)	6893 (4)	H8	682	371	534
C2	6849 (13)	5119 (9)	6664 (4)	H9	850	213	572
C3	6240 (12)	4009 (10)	6686 (4)	H10	1085	302	609
C4	7328 (14)	3342 (9)	6943 (4)	H11A	911	661	664
C5	8534 (13)	4028 (11)	7068 (4)	H11B	892	654	727
C6	9921 (15)	4598 (11)	5844 (5)	H12A	1142	662	703
C7	8565 (14)	4842 (10)	5588 (4)	H12B	1103	547	734
C8	7812 (15)	3812 (10)	5508 (4)	H13A	1153	439	667
C9	8736 (17)	2950 (10)	5719 (4)	H13B	1276	539	666
C10	10006 (16)	3433 (11)	5918 (5)	H14A	1202	530	579
C11	9247 (13)	6122 (9)	6952 (4)	H14B	1075	617	601
C12	10898 (15)	5881 (12)	7007 (5)	H15A	520	633	667
C13	11674 (14)	5199 (13)	6586 (6)	H15B	676	676	640
C14	11138 (14)	5385 (11)	6031 (5)	H16A	515	509	587
C15	6042 (13)	6118 (9)	6429 (4)	H16B	446	636	586
C16	5396 (13)	5906 (11)	5886 (5)	H17A	620	699	533
C17	6363 (14)	6185 (11)	5412 (5)	H17B	600	571	512
C18	8043 (13)	6007 (10)	5453 (4)	H18A	843	653	573
H3	525	376	655	H18B	849	621	511
H4	724	252	702				

[a] The non-hydrogen coordinates are multiplied by 10^4. The hydrogen coordinates are multiplied by 10^3. Since the coordinates of the hydrogens are not refined, the errors are not given.

The largest remaining peaks in I and II were near the β-carbons of the bridges. Other similar sized peaks were near the iron atoms.

No disorder was found in III, and the hydrogen atoms were all located on a difference map. The final full-matrix least-squares refinements were for the coordinates of the non-hydrogen atoms with anisotropic thermal parameters and of the hydrogen atoms with isotropic thermal parameters. The largest remaining peak was near an iron atom.

NMR spectra were obtained on a Bruker WH-360 spectrometer and on a JEOL MH-100 spectrometer in $CDCl_3$ solutions with Me_4Si as an internal standard. Redox potentials were measured vs. Ag/AgCl by cyclic voltammetry on an IBM EC/225 voltammetric analyzer, using ferrocene as an internal standard and 0.1 N Bu_4NClO_4 in CH_3CN as electrolyte and solvent.

Results

The atomic coordinates are given in Tables II, III, and IV. The thermal parameters and the observed and calculated structure factors are available as supplementary material. The molecular structures based on non-hydrogen atom coordinates are given in Figures 1, 2, and 3, respectively. Selected bond distances and angles are given in Tables V, VI, and VII. The least-squares planes of all of the rings and the dihedral angles between all pairs of planes are presented in Table VIII. The NMR spectra are given in Figure 4. All structures not included in Figures 1–4 are schematically given in Figure 5.

Discussion

We will address the consequences of four aspects of the structures of the title compounds and of related compounds: (1) iron-to-ring distance, (2) disorder, (3) ring–ring tilt and twist, and (4) other geometric phenomena. (Ring–ring tilt is defined as a deviation of the dihedral angle between the rings from 0°. Ring–ring twist is defined as the relative rotation of the two rings, where the twist angle is 0° for the eclipsed-ring conformation.)

Correlations of the iron-to-ring distances with the Mössbauer spectra[3] and with the redox potentials[4] have

Table III. Fractional Coordinates[a] for $C_{22}H_{28}Fe$ (II)

atom	x/a	y/b	z/c	atom	x/a	y/b	z/c
Fe1	26769 (3)	−23783 (3)	3356 (3)	Fe2	11061 (3)	24483 (3)	43488 (2)
C1	2851 (3)	−2522 (3)	1802 (2)	C23	1833 (3)	3382 (2)	5838 (2)
C2	3667 (3)	−1493 (3)	1802 (2)	C24	1613 (3)	4016 (2)	5140 (2)
C3	4643 (3)	−1676 (2)	1184 (2)	C25	178 (3)	3667 (2)	4626 (2)
C4	4458 (3)	−2790 (3)	784 (3)	C26	−496 (3)	2809 (2)	4969 (2)
C5	3359 (3)	−3306 (2)	1176 (2)	C27	513 (3)	2643 (2)	5730 (2)
C6	700 (3)	−2300 (3)	−73 (3)	C28	2772 (3)	1968 (2)	3995 (2)
C7	1662 (3)	−1406 (3)	−209 (3)	C29	2199 (3)	2424 (2)	3225 (2)
C8	2414 (3)	−1835 (3)	−932 (3)	C30	791 (3)	1805 (2)	2780 (2)
C9	1933 (4)	−2979 (3)	−1232 (3)	C31	484 (3)	986 (2)	3277 (2)
C10	881 (3)	−3230 (3)	−696 (3)	C32	1708 (3)	1074 (2)	4014 (2)
C11	1696 (4)	−2741 (3)	2340 (3)	C33	3154 (3)	3430 (3)	6548 (2)
C12	387 (4)	−3538 (4)	1664 (4)	C34	3501 (4)	2355 (3)	6437 (3)
C13	−703 (4)	−3137 (5)	1111 (5)	C35	4431 (3)	2078 (3)	5690 (3)
C14	−274 (4)	−2200 (4)	676 (4)	C36	4201 (3)	2354 (3)	4645 (3)
C15	3525 (4)	−424 (3)	2357 (3)	C37	2701 (3)	4880 (2)	4959 (3)
C16	3943 (4)	472 (3)	1880 (3)	C38	2416 (4)	5121 (3)	3916 (3)
C17	3369 (6)	388 (4)	792 (4)	C39	2106 (4)	4225 (3)	2914 (3)
C18	1858 (5)	−235 (3)	297 (5)	C40	2897 (4)	3368 (3)	2901 (3)
C19	5317 (4)	−3299 (3)	104 (3)	C41	−2004 (3)	2221 (3)	4627 (3)
C20	4500 (5)	−4086 (3)	−944 (3)	C42	−2321 (3)	998 (3)	4249 (3)
C21	3938 (4)	−3647 (4)	−1782 (3)	C43	−2143 (3)	529 (3)	3156 (3)
C22	2406 (5)	−3751 (4)	−2004 (3)	C44	−864 (3)	142 (3)	3066 (3)
H3	535	−111	105	H25	−28	398	411
H5	300	−410	104	H27	33	210	613
H8	316	−141	−119	H30	14	193	222
H10	34	−397	−75	H32	181	59	447
H11A	202	−302	293	H33A	393	393	640
H11B	147	−205	262	H33B	308	371	728
H12A	−6	−394	212	H34A	261	178	619
H12B	67	−404	112	H34B	397	235	714
H13A	−128	−375	51	H35A	541	246	607
H13B	−128	−293	161	H35B	431	129	553
H14A	−114	−209	30	H36A	482	204	423
H14B	20	−156	127	H36B	448	315	480
H15A	253	−51	239	H37A	282	555	551
H15B	411	−21	308	H37B	359	466	503
H16A	497	62	196	H38A	160	543	390
H16B	371	110	231	H38B	325	567	390
H17A	347	113	74	H39A	109	386	275
H17B	396	5	37	H39B	232	456	235
H18A	149	9	−25	H40A	383	371	338
H18B	131	−17	85	H40B	302	310	218
H19A	600	−272	−4	H41A	−245	240	523
H19B	583	−369	50	H41B	−243	247	404
H20A	369	−457	−80	H42A	−331	69	427
H20B	513	−451	−122	H42B	−169	77	474
H21A	443	−287	−159	H43A	−213	109	278
H21B	416	−402	−244	H43B	−297	−9	280
H22A	213	−364	−270	H44A	−102	−32	234
H22B	192	−449	−202	H44B	−76	−29	357

[a] The coordinates of the iron atoms are multiplied by 10^5. The coordinates of the carbon atoms are multiplied by 10^4. The coordinates of the hydrogen atoms are multiplied by 10^3. Since the coordinates of the hydrogen atoms are not refined, the errors are not given.

been established. For pentamethylene-bridged compounds it had been assumed that the iron-to-ring distances would be the same as in ferrocene (165 pm) since the pentamethylene bridge is long enough to span the two rings without strain. This has now been confirmed with the first crystal structure of a compound containing a pentamethylene bridge. The iron-to-ring distance in III, 164.7 (1) pm, is within 0.3 pm of the distance used for ferrocene in the correlation. The redox potential for III (not previously determined) is 110 mV vs. Ag/AgCl, in accord with the correlation previously reported.[4] The iron-to-ring distance for II, 162.9 (3) pm, had already been known at the time the correlation was made and was used accordingly. The iron-to-ring distance of I, 163.5 (1.0) pm, also fits the correlations with the Mössbauer parameters within the precision of the measurement.

These iron-to-ring distances suggest no explanation for the ring-proton anomalies in the NMR spectra of singly and doubly bridged ferrocenes. It is still possible, however, that such effects may be observed in the structures of singly bridged compounds and of the other dibridged compounds.

In all of the compounds for which there are isolated trimethylene bridges, disorder in the form of flipping of the isolated bridge has been found in bridge-proton region of the NMR spectra at room temperature. When there is a single trimethylene bridge as in IX and X,[16] the rate of flipping is so high that only a single sharp peak is found for the bridge protons. For two isolated trimethylene bridges as in V (Figure 4) and XI, two broad peaks are observed. Although the spectrum has not been analyzed rigorously, when the trimethylene bridges are adjacent as in XII, the spectrum (Figure 4) appears to be that of a

(16) Singletary, N. J.; Hillman, M. *Organometallics*, in press.

Table IV. Fractional Coordinates[a] for $C_{25}H_{34}Fe$ (III)

atom	x/a	y/b	z/c	atom	x/a	y/b	z/c
Fe	76755 (3)	−3449 (7)	95930 (3)	H11A	618 (2)	−65 (5)	1086 (2)
C1	7110 (2)	−2019 (5)	10364 (2)	H11B	626 (2)	−253 (5)	1120 (2)
C2	6732 (2)	−2370 (5)	9618 (2)	H12A	674 (2)	−40 (6)	1217 (2)
C3	7416 (2)	−2979 (5)	9160 (2)	H12B	742 (2)	−174 (5)	1199 (2)
C4	8221 (2)	−2972 (5)	9607 (2)	H13A	824 (2)	48 (5)	1132 (2)
C5	8025 (2)	−2417 (5)	10352 (2)	H13B	808 (2)	103 (5)	1213 (2)
C6	7450 (2)	2327 (5)	9953 (2)	H14A	790 (2)	364 (5)	1146 (2)
C7	7063 (2)	2044 (5)	9205 (2)	H14B	701 (2)	330 (5)	1181 (2)
C8	7754 (2)	1565 (5)	8724 (2)	H15A	642 (2)	243 (6)	1057 (2)
C9	8567 (2)	1485 (5)	9170 (2)	H15B	683 (3)	428 (6)	1051 (2)
C10	8364 (3)	1988 (6)	9920 (2)	H16A	554 (2)	−111 (5)	962 (2)
C11	6600 (3)	−1466 (6)	11034 (2)	H16B	551 (2)	−323 (5)	956 (2)
C12	7106 (3)	−710 (7)	11743 (2)	H17A	491 (2)	−197 (5)	847 (2)
C13	7759 (3)	890 (7)	11658 (2)	H17B	562 (2)	−325 (5)	831 (2)
C14	7410 (3)	2804 (7)	11406 (2)	H18A	655 (2)	−86 (5)	808 (2)
C15	6958 (3)	2982 (6)	10616 (2)	H18B	582 (2)	−87 (5)	754 (2)
C16	5769 (2)	−2197 (6)	9387 (2)	H19A	608 (3)	225 (6)	781 (2)
C17	5519 (3)	−2092 (7)	8533 (3)	H19B	518 (3)	161 (6)	818 (2)
C18	5952 (3)	−612 (7)	8060 (2)	H20A	598 (2)	352 (5)	895 (2)
C19	5773 (3)	1459 (7)	8221 (2)	H20B	577 (2)	174 (5)	938 (2)
C20	6108 (3)	2293 (6)	8978 (2)	H21A	957 (2)	−273 (5)	965 (2)
C21	9125 (2)	−3476 (6)	9371 (2)	H21B	929 (2)	−472 (5)	958 (2)
C22	9273 (3)	−3511 (7)	8523 (2)	H22A	987 (2)	−381 (5)	850 (2)
C23	9011 (3)	−1823 (7)	8039 (2)	H22B	898 (2)	−456 (6)	832 (2)
C24	9512 (3)	3 (7)	8159 (2)	H23A	843 (2)	−158 (5)	807 (2)
C25	9465 (2)	1028 (6)	8917 (2)	H23B	907 (2)	−222 (5)	748 (2)
H3	735 (2)	−329 (5)	864 (2)	H24A	930 (2)	88 (5)	778 (2)
H5	842 (2)	−231 (4)	1076 (2)	H24B	1009 (3)	−24 (6)	808 (2)
H8	769 (2)	132 (4)	820 (2)	H25A	979 (2)	37 (5)	933 (2)
H10	875 (2)	204 (4)	1035 (2)	H25B	979 (2)	209 (5)	889 (2)

[a] The coordinates of the iron atoms are multiplied by 10^5. The coordinates of the carbon atoms are multiplied by 10^4. The coordinates of the hydrogen atoms are multiplied by 10^3.

Table V. Selected Bond Distances (pm)

$C_{18}H_{22}Fe$ (I)		$C_{22}H_{28}Fe$ (II) unit I		$C_{22}H_{28}Fe$ (II) unit II		$C_{25}H_{34}Fe$ (III)	
Fe-C1	204 (1)	Fe1-C1	202.6 (3)	Fe2-C23	202.3 (3)	Fe-C1	203.6 (3)
Fe-C2	201 (1)	Fe1-C2	202.8 (2)	Fe2-C24	202.9 (3)	Fe-C2	204.1 (3)
Fe-C3	204 (1)	Fe1-C3	203.0 (3)	Fe2-C25	204.5 (3)	Fe-C3	205.6 (4)
Fe-C4	206 (1)	Fe1-C4	204.1 (3)	Fe2-C26	204.1 (3)	Fe-C4	204.8 (4)
Fe-C5	205 (1)	Fe1-C5	202.4 (4)	Fe2-C27	203.5 (3)	Fe-C5	204.2 (4)
Fe-C6	201 (1)	Fe1-C6	202.3 (3)	Fe2-C28	202.0 (3)	Fe-C6	204.2 (3)
Fe-C7	203 (1)	Fe1-C7	202.0 (4)	Fe2-C29	202.1 (3)	Fe-C7	204.1 (4)
Fe-C8	202 (1)	Fe1-C8	201.9 (4)	Fe2-C30	204.4 (3)	Fe-C8	205.7 (4)
Fe-C9	201 (1)	Fe1-C9	204.0 (3)	Fe2-C31	204.6 (2)	Fe-C9	205.5 (4)
Fe-C10	201 (1)	Fe1-C10	202.6 (3)	Fe2-C32	203.7 (3)	Fe-C10	203.3 (4)
C1-C2	140 (1)	C1-C2	144.2 (5)	C23-C24	143.3 (5)	C1-C2	142.7 (5)
C2-C3	143 (1)	C2-C3	142.0 (4)	C24-C25	142.9 (4)	C2-C3	142.3 (5)
C3-C4	142 (1)	C3-C4	142.0 (4)	C25-C26	141.8 (4)	C3-C4	142.2 (5)
C4-C5	139 (1)	C4-C5	142.2 (5)	C26-C27	142.4 (4)	C4-C5	141.8 (5)
C5-C1	142 (1)	C5-C1	143.1 (5)	C27-C23	144.2 (4)	C5-C1	142.8 (5)
C6-C7	141 (2)	C6-C7	143.7 (5)	C28-C29	143.5 (5)	C6-C7	142.7 (5)
C7-C8	142 (1)	C7-C8	142.9 (5)	C29-C30	143.5 (4)	C7-C8	143.2 (5)
C8-C9	143 (2)	C8-C9	143.8 (5)	C30-C31	141.9 (5)	C8-C9	143.3 (5)
C9-C10	137 (2)	C9-C10	140.8 (5)	C31-C32	142.6 (4)	C9-C10	142.0 (5)
C10-C6	141 (1)	C10-C6	139.9 (5)	C32-C28	143.3 (4)	C10-C6	142.2 (5)
C1-C11	147 (1)	C1-C11	148.8 (6)	C23-C33	149.7 (4)	C1-C11	150.4 (5)
C11-C12	151 (2)	C11-C12	150.8 (5)	C33-C34	153.3 (6)	C11-C12	153.0 (6)
C12-C13	152 (2)	C12-C13	150.1 (8)	C34-C35	152.9 (6)	C12-C13	152.7 (6)
C13-C14	152 (2)	C13-C14	151.6 (9)	C35-C36	154.1 (6)	C13-C14	152.1 (6)
C6-C14	152 (2)	C6-C14	152.9 (6)	C28-C36	148.1 (4)	C14-C15	152.3 (6)
						C6-C15	149.9 (5)
C2-C15	152 (1)	C2-C15	150.2 (5)	C24-C37	150.8 (4)	C2-C16	150.9 (5)
C15-C16	153 (1)	C15-C16	150.4 (6)	C37-C38	151.9 (6)	C16-C17	153.2 (6)
C16-C17	153 (1)	C16-C17	146.6 (7)	C38-C39	152.4 (5)	C17-C18	151.8 (6)
C17-C18	152 (1)	C17-C18	153.1 (6)	C39-C40	153.5 (6)	C18-C19	153.0 (6)
C7-C18	151 (2)	C7-C18	151.1 (5)	C29-C40	150.2 (5)	C19-C20	152.2 (6)
						C7-C20	150.2 (5)
		C4-C19	151.6 (5)	C26-C41	149.9 (4)	C4-C21	150.8 (5)
		C19-C20	153.7 (5)	C41-C42	153.9 (5)	C21-C22	152.4 (5)
		C20-C21	148.6 (7)	C42-C43	152.5 (6)	C22-C23	151.5 (5)
		C21-C22	150.3 (6)	C43-C44	150.9 (5)	C23-C24	151.8 (6)
		C9-C22	150.6 (6)	C31-C44	150.7 (4)	C24-C25	152.7 (5)
						C9-C25	150.2 (5)

Table VI. Bond Distances to Hydrogen Atoms for $C_{25}H_{34}Fe$ (III) (pm)

C3-H3	93 (3)	C5-H5	92 (3)	C8-H8	95 (3)
C10-H10	93 (3)	C11-H11A	91 (3)	C11-H11B	97 (4)
C12-H12A	98 (4)	C12-H12B	97 (4)	C13-H13A	101 (3)
C13-H13B	95 (3)	C14-H14A	96 (4)	C14-H14B	103 (4)
C15-H15A	92 (4)	C15-H15B	96 (4)	C16-H16A	96 (3)
C16-H16B	90 (4)	C17-H17A	93 (4)	C17-H17B	94 (4)
C18-H18A	92 (4)	C18-H18B	95 (4)	C19-H19A	105 (4)
C19-H19B	91 (4)	C20-H20A	90 (4)	C20-H20B	98 (3)
C21-H12A	98 (3)	C21-H21B	98 (4)	C22-H22A	94 (4)
C22-H22B	93 (4)	C23-H23A	90 (4)	C23-H23B	103 (4)
C24-H24A	95 (4)	C24-H24B	93 (4)	C25-H25A	98 (3)
		C25-H25B	90 (4)		

compound with rigid bridges. For the compound with three not-all-adjacent bridges, IV, the NMR spectrum is more complicated yet has some of the characteristics of the dibridged compounds with adjacent and nonadjacent bridges.

Compounds with bridges that do not flip rapidly, e.g., I, V, VI, XII, and XIX, have two groups of peaks of equal intensities. At −110 °C, the NMR spectrum of IX was also found to consist of two groups of peaks.[17] The occurrence of two groups of peaks is due to the approximate NMR equivalence of chemically nonequivalent hydrogens. On each α-carbon and on each β-carbon there is one C–H vector that is tangent to the iron atom and one C–H vector that points away from the iron atom, resulting in three of each kind of hydrogen on trimethylene bridges and four of each kind on tetramethylene bridges. We suggest that this is the origin of the two distinct groups.

NMR spectra of IV (Figure 4) are given at both 100 MHz and at 360 MHz. The peaks can be divided into three equal-area groups at 1.48, 1.81 and 2.14 ppm, respectively. The outer peaks are attributed to the adjacent trimethylene bridges that, as in XII, would normally not flip, and the central broad peak is attributed to the isolated trimethylene bridge that is flipping slowly. The motions of the rings associated with the flipping of the isolated bridge in IV, however, affect the adjacent bridges. This is reflected in the broadening of the outer peaks. There is a noticeable difference in the relative broadness of the three groups of peaks at the two different NMR frequencies of the measurements. This indicates that the rate of flipping is in that range that is measurable at the frequencies used. In principle, the widths of the central peaks at the two NMR frequencies may be used to obtain an approximate rate of flipping of the trimethylene group.

Those compounds with isolated trimethylene bridges for which the crystal structures have been determined, IV,[2] X,[18] and XI,[16] have been found to have disorder of the trimethylene bridges in the crystal structures as well, while those with trimethylene bridges adjacent to another group, XIII[19] and XIV,[16] have no discernible disorder in the trimethylene bridges. It has not been established whether the disorder in the crystals is dynamic or static. In solution it is, of course, dynamic.

The question of disorder in compounds with tetramethylene bridges is not as clearly resolved. The NMR spectra of compounds with isolated tetramethylene bridges have not been satisfactorily interpreted. They (VI and XIX in Figure 4) are neither the spectra expected for rapidly flipping bridges nor the spectra expected for nonflipping bridges (compound I in Figure 4 gives the expected spectrum for nonflipping tetramethylene bridges). The situation is probably somewhere in between, involving some motion of the bridges. By virtue of the persistence of residual electron density in the neighborhood of the tetramethylene bridges of I and II, a small amount of disorder is also believed to exist in the bridges in the crystals. The foreshortened C–C bonds observed for the bridges are also indicative of disorder or large thermal motion. Similarly it is reported that the determination of the structure of XV[20] was troubled by the existence of disorder and foreshortened bonds in the bridges. Neither phenomenon was observed for XVI[21] and XVII,[22] however. Compound XVIII[23] was found to have rotational disorder.

The NMR spectrum of VIII at 360 MHz (Figure 4) reveals that the pentamethylene bridge is flipping rapidly. The expected triplet and two quintets are readily discerned. On the other hand, and in contrast to the NMR spectrum of IV, which shows flipping at a much slower rate than in IX, the NMR spectrum of III has a complex coupling scheme and is that of a much more rigid molecule.[24] Since the pentamethylene bridge is expected to be the most flexible of the three, this is surprising. Consistent with this observation, no disorder of a bridge was found in the crystal structure of III. This indicates that, in the solid state, at least, a preferred conformation exists for the bridges. The conformation found is not the one that would have been predicted by using simple models since these lead to a close approach of a γ-proton and the iron. In the actual crystal, the removal of the proton from the iron is accomplished by distortion of the bond angles in the bridge. Since the observed conformation is that of the smallest volume and hence of the densest packing, its occurrence might be attributed to lattice effects. That this is not the best explanation is described in the next paragraphs.

In the solid state, the angle that the cyclopentadienyl rings of ferrocene twist with respect to each other is[25-27] about 9–12°. As a gas, and presumably in solution, the preferred conformation is eclipsed.[28] It would be expected then that, in the absence of strain, the twist angle of derivatives of ferrocene should be nearly eclipsed. However, the energy barrier to rotation is so low, 0.9 kcal, that the effect of eclipsing vs. staggering is not otherwise observable in ferrocene derivatives without rotational hindrance.

A trimethylene bridge is too short, even when extended, to span the distance between the cyclopentadienyl rings of ferrocene. Strain introduced into the molecule is exhibited in several ways. The rings are forced to be eclipsed, and the rings are tilted and pulled closer to each other. With three not-all-adjacent trimethylene bridges, IV, the tilting (2.5°) is almost completely eliminated,[2] and the rings are closer (157.3 (2) pm) than in any other known ferrocene derivative. The twist angle of the rings is 0.6 (6)°. A high degree of strain has been demonstrated for this molecule

(17) Abel, E. W.; Booth, M.; Brown, C. A.; Orrell, K. G.; Woodford, R. L. *J. Organomet. Chem.* **1981**, *214*, 93–105.
(18) Hillman, M.; Gordon, B.; Dudek, N.; Fajer, R.; Fujita, E.; Gaffney, J.; Jones, P.; Weiss, A. *J. Organomet. Chem.* **1980**, *194*, 229–256.
(19) Hillman, M.; Fujita, E. *J. Organomet. Chem.* **1978**, *155*, 99–108.
(20) Hisatome, M.; Kawaziri, Y.; Yamakawa, K. *Tetrahedron Lett.* **1979**, 1777–1780.
(21) Hisatome, M.; Kawajiri, Y.; Yamakawa, K.; Kozawa, K.; Uchida, T. *J. Organomet. Chem.* **1982**, *236*, 359–365.
(22) Struchkov, Yu. T.; Aleksandrov, G. G.; Kreindlin, A. Z.; Rybinskaya, M. I. *J. Organomet. Chem.* **1981**, *210*, 237–245.
(23) Hisatome, M.; Kawajiri, Y.; Yamakawa, K.; Harada, Y.; Iitaka, Y. *Tetrahedron Lett.* **1982**, *23*, 1713–1716.
(24) Hisatome, M., unpublished results.
(25) Seiler, P.; Dunitz, J. D. *Acta Crystallogr., Sect. B* **1979**, *B35*, 1068–1074.
(26) Takusagawa, F.; Koetzle, T. F. *Acta Crystallogr., Sect. B* **1979**, *B35*, 1074–1081.
(27) Clec'h, G.; Calvarin, G.; Berar, J. F.; Andre, D. *C. R. Hebd. Seances Acad. Sci., Ser. C* **1978**, *287*, 523–525.
(28) Haaland, A.; Nilsson, J. E. *J. Chem. Soc., Chem. Commun.* **1968**, 88–89.

Table VII. Selected Bond Angles (deg)

$C_{18}H_{22}Fe$ (1)		$C_{22}H_{28}Fe$ (II) unit I		$C_{22}H_{28}Fe$ (II) unit II		$C_{25}H_{34}Fe$ (III)	
C1-C2-C3	110 (1)	C1-C2-C3	107.2 (3)	C23-C24-C25	107.8 (2)	C1-C2-C3	107.7 (3)
C2-C3-C4	106 (1)	C2-C3-C4	109.9 (3)	C24-C25-C26	109.2 (3)	C2-C3-C4	109.0 (3)
C3-C4-C5	108 (1)	C3-C4-C5	106.5 (3)	C25-C26-C27	107.2 (2)	C3-C4-C5	107.0 (3)
C4-C5-C1	110 (1)	C4-C5-C1	109.5 (3)	C26-C27-C23	109.0 (3)	C4-C5-C1	109.1 (3)
C5-C1-C2	106 (1)	C5-C1-C2	106.9 (3)	C27-C23-C24	106.8 (2)	C5-C1-C2	107.3 (3)
C6-C7-C8	107 (1)	C6-C7-C8	106.6 (3)	C28-C29-C30	107.7 (3)	C6-C7-C8	107.5 (3)
C7-C8-C9	107 (1)	C7-C8-C9	109.0 (3)	C29-C30-C31	108.6 (3)	C7-C8-C9	109.2 (3)
C8-C9-C10	109 (1)	C8-C9-C10	106.1 (3)	C30-C31-C32	107.7 (2)	C8-C9-C10	105.8 (3)
C9-C10-C6	109 (1)	C9-C10-C6	110.5 (3)	C31-C32-C28	108.7 (3)	C9-C10-C6	110.3 (3)
C10-C6-C7	108 (1)	C10-C6-C7	107.9 (3)	C32-C28-C29	107.3 (2)	C10-C6-C7	107.1 (3)
C5-C1-C11	128 (1)	C5-C1-C11	125.9 (3)	C27-C23-C33	124.6 (3)	C5-C1-C11	128.0 (3)
C2-C1-C11	127 (1)	C2-C1-C11	127.2 (3)	C24-C23-C33	128.6 (3)	C2-C1-C11	124.6 (3)
C1-C2-C15	126 (1)	C1-C2-C15	126.7 (3)	C23-C24-C37	126.3 (2)	C1-C2-C16	124.8 (3)
C3-C2-C15	124 (1)	C3-C2-C15	126.1 (3)	C25-C24-C37	125.9 (3)	C3-C2-C16	127.5 (3)
		C3-C4-C19	125.5 (3)	C25-C26-C41	126.3 (3)	C3-C4-C21	128.6 (3)
		C5-C4-C19	128.0 (3)	C27-C26-C41	126.5 (3)	C5-C4-C21	124.4 (3)
C10-C6-C14	122 (1)	C10-C6-C14	128.2 (3)	C32-C28-C36	126.7 (3)	C10-C6-C15	128.4 (4)
C7-C6-C14	130 (1)	C7-C6-C14	123.9 (3)	C29-C28-C36	126.0 (3)	C7-C6-C15	124.3 (3)
C6-C7-C18	124 (1)	C6-C7-C18	127.8 (4)	C28-C29-C40	128.2 (2)	C6-C7-C20	125.0 (3)
C8-C7-C18	128 (1)	C8-C7-C18	125.7 (3)	C30-C29-C40	124.1 (3)	C8-C7-C20	127.4 (3)
		C8-C9-C22	127.0 (4)	C30-C31-C44	127.5 (3)	C8-C9-C25	128.6 (3)
		C10-C9-C22	126.8 (4)	C32-C31-C44	124.7 (3)	C10-C9-C25	125.6 (3)
C1-C11-C12	116 (1)	C1-C11-C12	114.7 (3)	C23-C33-C34	114.5 (2)	C1-C11-C12	118.2 (3)
C11-C12-C13	119 (1)	C11-C12-C13	118.7 (4)	C33-C34-C35	117.2 (3)	C11-C12-C13	119.0 (3)
C12-C13-C14	116 (1)	C12-C13-C14	119.7 (4)	C34-C35-C36	118.5 (3)	C12-C13-C14	118.6 (3)
C13-C14-C6	116 (1)	C13-C14-C6	116.8 (4)	C35-C36-C28	116.9 (3)	C13-C14-C15	118.3 (4)
						C14-C15-C6	117.7 (4)
C2-C15-C16	114 (1)	C2-C15-C16	116.6 (3)	C24-C37-C38	116.8 (2)	C2-C16-C17	116.9 (3)
C15-C16-C17	118 (1)	C15-C16-C17	122.1 (3)	C37-C38-C39	119.7 (3)	C16-C17-C18	118.7 (4)
C16-C17-C18	118 (1)	C16-C17-C18	119.4 (5)	C38-C39-C40	117.6 (3)	C17-C18-C19	118.8 (4)
C17-C18-C7	117 (1)	C17-C18-C7	114.1 (4)	C39-C40-C29	114.9 (3)	C18-C19-C20	118.9 (4)
						C19-C20-C7	117.4 (3)
		C4-C19-C20	115.7 (3)	C26-C41-C42	115.6 (3)	C4-C21-C22	117.6 (3)
		C19-C20-C21	118.2 (4)	C41-C42-C43	116.5 (3)	C21-C22-C23	119.3 (4)
		C20-C21-C22	117.2 (4)	C42-C43-C44	117.2 (3)	C22-C23-C24	119.1 (4)
		C21-C22-C9	115.2 (3)	C43-C44-C31	116.6 (3)	C23-C24-C25	119.0 (4)
						C24-C25-C9	116.9 (4)

Table VIII. Least-Squares Planes

Equations for Distances from Planes (pm)

$C_{18}H_{22}Fe$ (I)

ring I: C1-C5 — $D = 375.44x - 257.71y - 2261.1z + 1381.0$
ring II: C6-C10 — $D = 404.69x - 119.15y - 2273.0z + 981.34$

$C_{22}H_{28}Fe$ (II)

ring I: C1-C5 — $D = -557.41x + 445.38y - 998.39z + 451.46$
ring II: C6-C10 — $D = -608.09x + 508.83y - 939.56z + 152.76$
ring III: C23-C27 — $D = 506.59x - 769.05y - 860.80z + 669.95$
ring IV: C28-C32 — $D = 583.99x - 723.02y - 865.10z + 325.58$

$C_{25}H_{34}Fe$ (III)

ring I: C1-C5 — $D = 275.28x + 677.48y - 460.44z + 418.46$
ring II: C6-C10 — $D = 246.22x + 688.00y - 374.25z + 29.124$

Distances of Iron Atoms from Planes (ppm)

$C_{18}H_{22}Fe$ (I)	Fe	164.5 (1)	162.5 (1)			
$C_{22}H_{28}Fe$ (II)	Fe1	162.9 (1)	162.5 (1)	Fe2	163.3 (1)	163.1 (1)
$C_{25}H_{34}Fe$ (III)	Fe	164.7 (1)	164.6 (1)			

Angles between Planes (deg)

$C_{18}H_{22}Fe$ (I)	ring I-ring II	6.9		
$C_{22}H_{28}Fe$ (II)	ring I-ring II	4.5	ring III-ring IV	5.5
$C_{25}H_{34}Fe$ (III)	ring I-ring II	3.1		

by the opening of bridges by strong acids.[18,29]

The tetramethylene bridge appears to be long enough to span the rings. Hisatome[21] has suggested that it is too long to span the rings without introducing ring–ring twisting and/or tilting into the molecule. In I and II, the twist angles were found to be 12–14°. This can be interpreted as consistent with Hisatome's suggestion that the tetramethylene bridge needs more room and consequently staggers the rings a little to achieve it, but a different explanation seems more appropriate.

Since a pentamethylene bridge is even longer than a tetramethylene bridge, it should by analogy induce even more twisting. Nesmeyanov[30] has suggested that a twist

(29) Hillman, M.; Gordon, B.; Weiss, A. J.; Guzikowski, A. P. *J. Organomet. Chem.* **1978**, *155*, 77–86.

of up to 72° could explain the NMR spectrum of IV. The crystal structure of III, however, reveals that the compound with three pentamethylene bridges is eclipsed. The measured twist angle is 0.7 (1)°. Thus, the length of the bridge is not the major determinant for staggering or eclipsing the cyclopentadienyl rings.

The feature that appears to be the driving force is the arrangement of the protons of the bridges. It is apparent from models that an eclipsed conformation of the rings for a molecule containing a tetramethylene bridge forces the proton on the bridge to be eclipsed with resulting short hydrogen–hydrogen distances. This is relieved by twisting the rings by the 12–14° observed in I and II. On the other hand, twisting of the rings in a compound containing a pentamethylene bridge forces the protons on the bridge to have a much higher probability of interaction than when the rings are eclipsed. With eclipsed rings, there are several possible conformations for a pentamethylene bridge. From models it can be seen that the conformation that gives the least eclipsing of the bridge protons is the one used by all of the bridges in III. The repulsion of the γ-proton by the iron is more easily alleviated by enlarging the bond angles.

While extrapolating from crystal structures to phenomena in solution is dangerous, an intramolecular interaction would be common to both. Conformations that avoid eclipsing of protons are expected to occur in solutions as well as in crystals. Thus, there is a high likelihood that the predominant pentamethylene conformation in solution is the same as observed in the crystal structure of III. In the case of V, however, the ease of conversion of this conformation to others is indicated by the rapid flipping observed in the NMR spectrum of V.

It is possible that the staggered conformation of the rings that is observed in tetramethylene-bridged ferrocenes is a source of the anomalous arrangement of the ring-proton peaks in the NMR spectra of bridged ferrocenes. Additional evidence is required.

Acknowledgment. We are indebted to Dr. A. McLaughlin and Mr. D. Lawler for the NMR spectra at 360 MHz. We are indebted to Dr. A. C. Larson for helpful discussions. This work was supported by the Division of Chemical Sciences, U.S. Department of Energy, Washington, D.C., under Contract No. DE-AC02-76CH00016.

Registry No. I, 75827-48-4; II, 72177-38-9; III, 79169-89-4; IV, 56045-61-5.

Supplementary Material Available: Tables of anisotropic thermal parameters and structure factors for $FeC_{18}H_{22}$, $FeC_{22}H_{28}$, and $FeC_{25}H_{34}$ and isotropic thermal parameters for $FeC_{25}H_{34}$ (51 pages). Ordering information is given on any current masthead page.

(30) Nesmeyanov, A. N.; Shul'pin, G. B.; Petrovskii, P. V.; Robas, B. I.; Rybinskaya, M. I. *Dokl. Akad. Nauk SSSR* 1974, *215*, 865–868.

Thermally Induced Diastereoisomerization of (Cyclobutadiene)cobalt Complexes as a Probe for the Reversibility of Their Formation from Complexed Alkynes

Guy A. Ville,[1a,c] K. Peter C. Vollhardt,*[1a] and Mark J. Winter*[1a,b]

Department of Chemistry, University of California, Berkeley, the Materials and Molecular Research Division, Lawrence Berkeley Laboratory, Berkeley, California 94720, and the Department of Chemistry, The University, Sheffield, S3 7HF United Kingdom

Received February 6, 1984

The synthesis and separation of a series of racemic diastereomers **2–5** of formula Co[η^4-C(SiMe$_3$)C(SiMe$_3$)CHCCHMeR](η-C$_5$H$_5$) by cocyclization of Co(CO)$_2$(η-C$_5$H$_5$), Me$_3$SiC$_2$SiMe$_3$ (btmse), and HC$_2$CHMeR are described. Gas- and solution-phase pyrolyses for both diastereomers of Co[η^4-C(SiMe$_3$)C(SiMe$_3$)CHCCHMePh](η-C$_5$H$_5$) (**5**) reveal extensive mutual interconversion. A crossover experiment demonstrates the unimolecular character of this reaction and studies on enantiomerically enriched Co[η^4-C(SiMe$_3$)C(SiMe$_3$)CHCCHMeOH](η-C$_5$H$_5$) (**2**) show that the cobalt unit is the site of diastereoisomerization rather than the alternative carbon chiral center. During gas-phase pyrolysis of **5** small amounts of the geometrical isomer Co[η^4-C(SiMe$_3$)CHC(SiMe$_3$)CCHMePh](η-C$_5$H$_5$) (**12**) are formed. Similarly, gas-phase pyrolysis of **12** results in a small extent of positional isomerization to both diastereomers of **5**. Heating one diastereomer of **26**, i.e., Co[η^4-C(SiMe$_3$)C(SiEt$_3$)CHCCHMePh](η-C$_5$H$_5$) (**26a**), results in one diastereomer of **27**, Co[η^4-C(SiEt$_3$)C(SiMe$_3$)CHCCHMePh](η-C$_5$H$_5$) (**27b**), but *none* of **26b**. An experiment utilizing the 1,2-^{13}C-labeled cyclobutadiene **26a** results only in 1,3-^{13}C-labeled **27b**. The results are best interpreted by assuming that the cyclobutadiene rings open directly to bis(alkyne)cobalt species *without* the intermediacy of cobaltacyclopentadiene intermediates. Alternative rationales are discussed.

Introduction

By what mechanisms are metal cyclobutadiene complexes formed from alkynes? To what extent are such transformations reversible? This paper addresses these questions for cyclopentadienylcobalt chemistry.[2]

Interactions of transition-metal compounds with alkynes lead to many types of complexes. Among them those

(1) (a) University of California. (b) University of Sheffield. (c) Current address: C.N.R.S. ER84, Université Pierre and Marie Curie 75005, Paris, France.

0276-7333/84/2303-1177$01.50/0